

Photonic crystal properties of packed submicrometric SiO₂ spheres

H. Míguez, C. López,^{a)} F. Meseguer, A. Blanco, L. Vázquez, and R. Mayoral
*Instituto de Ciencia de Materiales de Madrid (CSIC), Cantoblanco, 28049 Madrid, Spain, and
Dep. Física Aplicada., Unidad Asociada (CSIC-UPV), 46022 Valencia, Spain*

M. Ocaña

Instituto de Ciencia de Materiales de Sevilla (CSIC), 41012 Sevilla, Spain

V. Fornés and A. Mifsud

Instituto de Tecnología Química (UPV-CSIC), 46022 Valencia, Spain

(Received 2 December 1996; accepted for publication 2 July 1997)

In this letter, we investigate the optical properties of packed monodisperse silica submicron spheres by means of optical transmission measurements. The results are compatible with a three dimensional face centered cubic order in these solid structures. The lattice parameter of these structures, and therefore their optical properties, can be easily tuned through the sphere size (between 200 and 700 nm) thus covering the whole visible and near infrared spectrum. © 1997 American Institute of Physics. [S0003-6951(97)00935-2]

Photonic band gap materials have gathered great importance in recent years.¹⁻³ Some photoelectronic devices,⁴ as lasers, can dramatically increase their efficiency because the coupling between electronic and light states can be advantageously modified. A great effort has already been put in theoretical calculations.⁵ It is very desirable to obtain three dimensional (3D) photonic crystals for the visible range of the electromagnetic spectrum. So far experiments on 3D structures are mostly restricted to the millimeter and submillimeter regions where photonic crystals with full gap have been obtained in different ranges.⁶ In two dimensional structures, a wider range has been covered, including the visible.⁷ Very few experiments on 3D photonic band gap solid structures in the visible region have been reported,⁸ these having only a very restricted number of layers.

Three-dimensional periodic dielectric structures have so far been achieved through the self-ordering in suspensions of latex microparticles. These colloidal crystals show Bragg diffraction effects in the optical region of the spectrum⁹ and optical evidence of the 3D face centered cubic (fcc) ordering has been found.¹⁰ However, these sorts of systems are very unmanageable as they are liquid suspensions.

The use of opal-like structures as photonic crystals was recently proposed.^{11,12} Opals are natural 3D close packed arrangements of amorphous silica spheres.¹³

In this letter, we investigate the optical properties of packed monodisperse silica spheres. Solid samples are obtained from a colloidal suspension of microspheres. The spheres employed have less than 5% of dispersion in diameter. The growth of the crystalline phase takes place close to equilibrium and can be described by the Edwards–Wilkinson model.¹⁴ Since the as-grown samples present a small cohesion, a sintering process is performed in order to improve their mechanical properties. In green samples, spheres are kept in place by van der Waals forces, whereas in the sintered ones the spheres are joined together by the formation of intersphere necks. Full details of the fabrication can be found elsewhere.¹⁵ As the structures are close packed, the lattice

parameter of the samples can be varied (between 200 and 700 nm) through the sphere diameter.

Scanning electron microscopy (SEM) and atomic force microscopy (AFM) in tapping mode is used to study the surface. Thus, surface quality and sphere size are characterized. In Fig. 1, a SEM image from the top surface of a sample made with spheres of 415 nm is shown. The triangular arrangement observed can correspond, in principle, to either a (111) surface of a fcc system or a (001) surface of a hexagonal close packed (hcp) one. Recently, Van Blaaderen *et al.* have grown fcc sphere packings through a template directed crystallization.¹⁶ The SEM and AFM images reveal that the surface presents large ordered domains ($\sim 20 \mu\text{m}$ across in average¹⁴ and up to hundreds of μm in some cases). At longer range, domains are observed with slightly different orientations due to defects such as steps, vacancies, and dislocations as can be seen in ordinary atomic solids.

The ordering of the submicrometric spheres in the growth direction has been investigated as well. A typical SEM photograph of a cleaved edge is shown in Fig. 2. Here one can see that vertical order has coherence lengths of tens of microns. Wide sections with triangular arrangements corresponding to {111} planes can be observed. This sort of

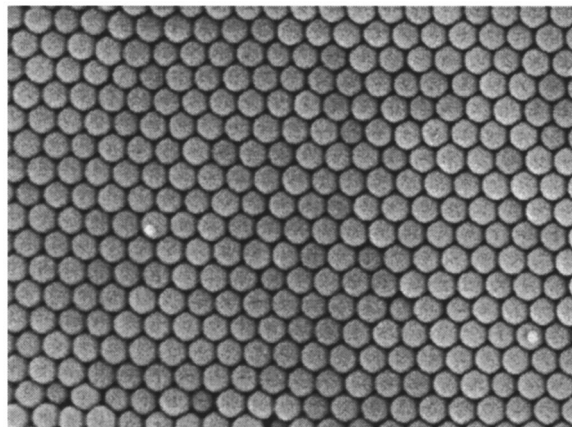


FIG. 1. SEM image of a $6 \times 10 \mu\text{m}^2$ region of the surface of a sample made from 415 nm spheres.

^{a)}Corresponding author. Electronic mail: cefe@icmm.csic.es

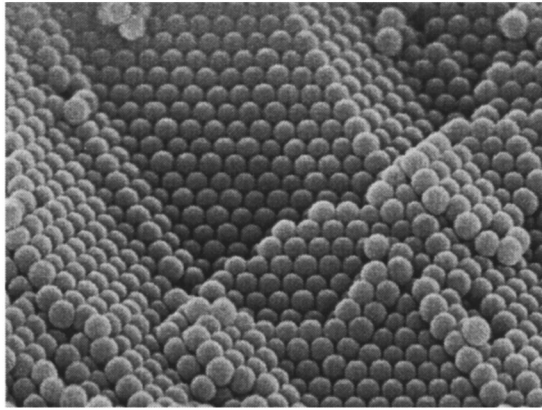


FIG. 2. SEM image from a cleaved edge. $(\bar{1}\bar{1}1)$ and $(11\bar{1})$ surfaces can be seen.

lateral order can only be seen if the spheres are arranged in an fcc structure. The two surfaces which can be seen in Fig. 2 correspond to $(\bar{1}\bar{1}1)$ and $(11\bar{1})$ crystalline planes of an fcc structure.

In order to optically characterize these structures, light transmission measurements were performed. In transmission spectra, information on every Bragg diffracting plane is contained. As samples have an average thickness of the order of 1 mm, thousands of layers are crossed by the transmitted radiation. The sample surface tested was 30 mm².

In Fig. 3, the spectra recorded for samples made of spheres with different diameter (from 220 to 535 nm) are shown. These spectra were measured at normal incidence ($\theta=0^\circ$). A clear attenuation band in the optical transmission can be observed in each case due to the Bragg reflection caused by the (111) planes. As the sphere size decreases, the Bragg reflection moves linearly towards shorter wavelengths (see Fig. 3). This shows the accurate tuning of the optical properties resulting from the sphere size control.

In Fig. 4, the Bragg reflection maximum (λ_c) has been plotted against the sphere size (ϕ). We can fit λ_c using Bragg

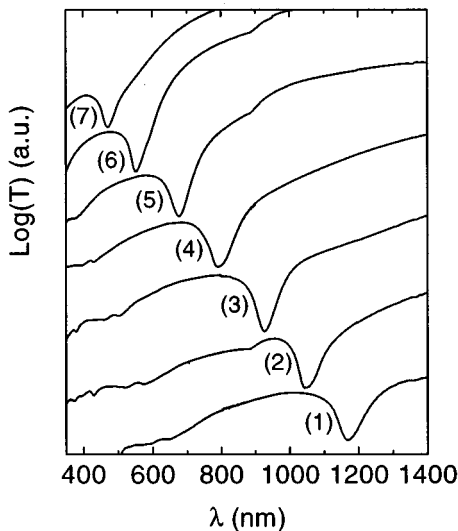


FIG. 3. Optical transmission at $\theta=0^\circ$ for opal-like structures made of spheres with different diameter: (1) 535, (2) 480, (3) 415, (4) 350, (5) 305, (6) 245, and (7) 220 nm. Spectra have been vertically shifted for the sake of clarity.

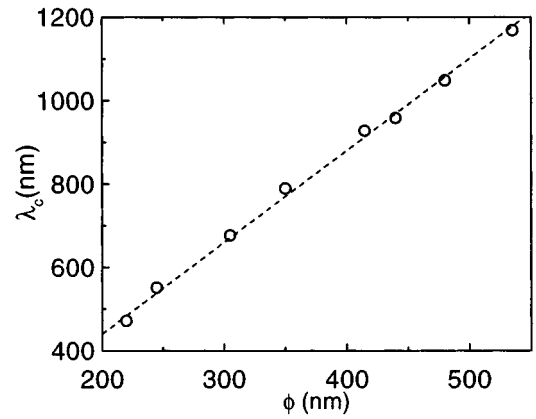


FIG. 4. The Bragg reflection maximum wavelength (λ_c) plotted against the sphere size and fit to Bragg law (dashed line).

law for normal incidence: $\lambda_c=2 \cdot n \cdot d$, where n is the effective index of refraction of the SiO_2/air composite and $d=0.816 \cdot \phi$ the distance between crystalline planes in the direction $\theta=0^\circ$. Thus from the slope of the fitted curve (dashed line in Fig. 4), we obtain $n=1.349$, which is extremely close to $n=1.348$, the value obtained averaging the dielectric constant $\epsilon=(n_1)^2 f+(n_2)^2(1-f)$, where f is the filling factor ($f=0.74$ for a close packed structure).

In order to estimate peak broadening effects, we have compared our experimental results with the analytical expression derived by Tarhan and Watson.¹⁷ In their model, $(\Delta\omega/\omega_c)=0.054$ for the $[111]$ stop band of an fcc photonic crystal.¹⁸ The experimental $(\Delta\omega/\omega_c)$ is larger in all cases (0.08 in average), which can in principle be due to the existence of domains.

Transmission measurements of visible and near infrared (NIR) radiation were also performed at different angles θ

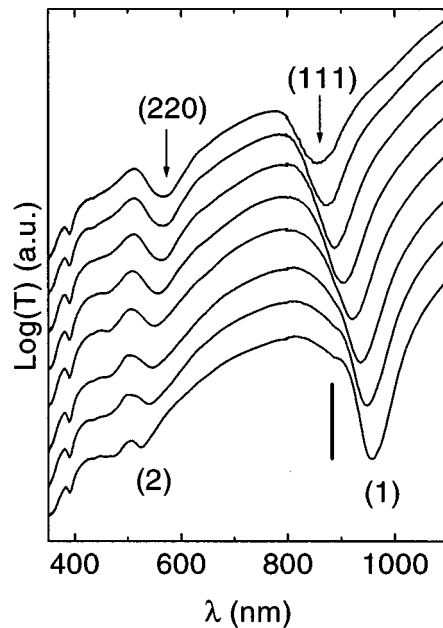


FIG. 5. Transmission spectra for different incidence angles, θ with respect to the surface normal in a sample made of 440 nm diameter spheres. From bottom to top, $\theta=0^\circ, 10^\circ, 15^\circ, 20^\circ, 25^\circ, 30^\circ, 35^\circ$, and 40° . The vertical bar indicates one decade. Spectra have been vertically shifted for the sake of clarity.

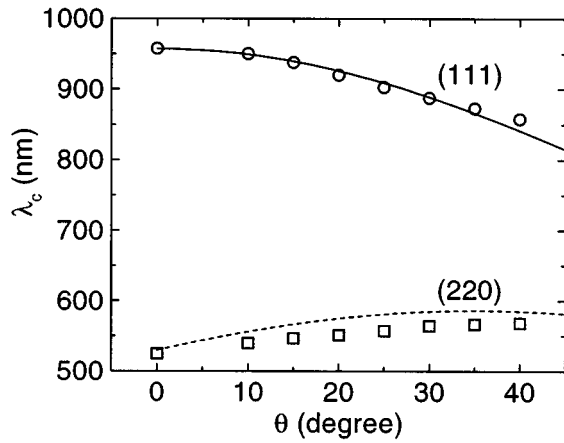


FIG. 6. λ_c of the [111] and [220] bands plotted against θ (circles and squares, respectively) and their calculated angular dependence in a cubic close packing (solid and dashed line, respectively).

with respect to the surface normal. The results obtained for a sample formed by spheres of 440 nm diam, (according to AFM), are shown in Fig. 5. No difference was found between TE and TM polarized light.

At normal incidence ($\theta=0^\circ$), a clear attenuation band corresponding to the [111] Bragg reflection can be observed [band (1) centered at 957.5 nm], along with a weaker dip [band (2) centered at 525 nm]. As the angle increases, band (1) shifts to shorter wavelengths according to the Bragg law while band (2) shifts to longer wavelength. The latter band can be explained as a [220] reflection. This behavior is summarized in Fig. 6, where both peaks' wavelengths are plotted against θ along with the calculated angular dependence of the [111] and [220] Bragg reflections (solid and dashed lines, respectively) of an fcc structure. We have considered $\phi = 440$ nm, as measured by AFM, and $n = 1.348$.

Thus, although the arrangement of layers can follow either fcc or hcp structure, both scanning electron microscopy (SEM) photographs and transmission measurements indicate that the cubic one could be favored. This tendency to the fcc arrangement has been observed before in colloidal crystals of latex particles slowly grown from dilute suspensions.¹⁹

In summary, we show that packings of SiO₂ submicron spheres, whose optical properties are investigated in this letter, are 3D photonic crystals in the visible and near infrared. Microscopy and optical evidence of the 3D ordering has been found that strongly supports an fcc structure. We observe pseudogaps or nonoverlapping gaps because our photonic crystal has a refractive index contrast of about 1.45 and a filling factor of 74%. The lattice parameter, and therefore

the optical properties, can be controlled through the size of the spherical particles.

These structures can be used as matrices to host high refractive index materials in order to obtain a full photonic band gap material. For a close packed fcc structure with $n_2/n_1 = 4$, the appearance of a full band gap between the 8th and 9th photonic bands has been predicted.²⁰

The authors would like to thank J. L. Sacedón for encouragement and M. Planes and M. J. Lacruz for SEM characterization. This work was partially financed by the Spanish CICyT, Project No. MAT94-0727, the EU under the Human Capital and Mobility Program, Contract No. CHRX-CT94-0464, and the Fundación Ramón Areces.

- ¹E. Yablonovitch, Phys. Rev. Lett. **58**, 2059 (1987).
- ²S. John, Phys. Rev. Lett. **58**, 2486 (1987).
- ³J. D. Joannopoulos, R. D. Meade, and J. N. Winn, *Photonic Crystals* (Princeton University Press, Princeton, NJ, 1995).
- ⁴J. D. Joannopoulos, P. R. Villeneuve, and Shanhui Fan, Nature (London) **386**, 143 (1997).
- ⁵*Photonic Band Gap Materials*, edited by C. M. Soukoulis (NATO ASI Series E: Applied Sciences), Vol. 315.
- ⁶E. Yablonovitch, T. J. Gmitter, and K. M. Leung, Phys. Rev. Lett. **67**, 2295 (1991); E. Özbay, G. Tuttle, M. Sigalas, C. M. Soukoulis, and K. M. Ho, Phys. Rev. B **51**, 13 961 (1995); E. Özbay, E. Michel, G. Tuttle, R. Biswas, K. M. Ho, J. Bostak, and D. M. Bloom, Opt. Lett. **19**, 1155 (1994).
- ⁷A. Rosenberg, R. J. Tonucci, and E. A. Bolden, Appl. Phys. Lett. **69**, 2638 (1996); H. B. Lin, R. J. Tonucci, and A. J. Campillo, Appl. Phys. Lett. **68**, 2927 (1996); K. Inoue, M. Wada, M. Hayashi, T. Fukushima, and A. Yamanka, Phys. Rev. B **53**, 1010 (1996); U. Grünig, V. Lehmann, and C. M. Engelhart, Appl. Phys. Lett. **66**, 3254 (1996).
- ⁸C. C. Cheng and A. Scherer, J. Vac. Sci. Technol. B **13**, 2696 (1995).
- ⁹P. A. Hiltner and I. M. Krieger, J. Phys. Chem. **73**, 2386 (1969).
- ¹⁰I. I. Tarhan and G. H. Watson, Phys. Rev. Lett. **76**, 315 (1996).
- ¹¹C. López, H. Míguez, L. Vázquez, F. Meseguer, R. Mayoral, and M. Ocaña, Superlattices Microstruct. (in press).
- ¹²V. N. Bogomolov, S. V. Gaponenko, A. M. Kapitonov, A. V. Prokofiev, S. M. Samoilovich, A. N. Ponyavina, and N. L. Silvanovich, *The Physics of Semiconductors*, edited by M. Scheffler and R. Zimmermann (World Scientific, Singapore, 1996), Vol. 4, p. 3139.
- ¹³J. V. Sanders, Nature (London) **204**, 1151 (1964).
- ¹⁴R. C. Salvarezza, L. Vázquez, H. Míguez, R. Mayoral, C. López, and F. Meseguer, Phys. Rev. Lett. **77**, 4572 (1996).
- ¹⁵R. Mayoral, J. Requena, S. J. Moya, C. López, A. Cintas, H. Míguez, F. Meseguer, L. Vázquez, M. Hologado, and A. Blanco, Adv. Mater. **9**, 257 (1997).
- ¹⁶A. van Blaaderen, R. Ruel, and P. Wiltzius, Nature (London) **385**, 321 (1997).
- ¹⁷I. I. Tarhan and G. H. Watson, Phys. Rev. B **54**, 7593 (1996).
- ¹⁸Although their model is based on scalar wave approximation, the results for the (111) stop band have been shown to be in fairly good agreement with a full vector wave calculation.
- ¹⁹P. N. Pusey, W. van Meegen, P. Bartlett, B. J. Ackerson, J. G. Rarity, and S. M. Underwood, Phys. Rev. Lett. **63**, 2753 (1989).
- ²⁰H. S. Sözüer and J. W. Haus, Phys. Rev. B **45**, 13 962 (1992).